Infrared Transmission Spectra for Extrasolar Giant Planets

Giovanna Tinetti[1,2]

tinetti@iap.edu

Mao-Chang Liang[3,4]

mcl@gps.caltech.edu

Alfred Vidal-Madjar [2]

alfred@iap.fr

David Ehrenreich [2]

ehrenreich@iap.fr

Alain Lecavelier des Etangs [2]

lecaveli@iap.fr

and

Yuk L. Yung[3]

yly@gps.caltech.edu

[1] European Space Agency

[2] Institut d'Astrophysique de Paris, CNRS (UMR 7095), Université Pierre et Marie Curie, 75014 Paris, France

[3] California Institute of Technology, Division of Geological and Planetary Sciences, Pasadena, CA 91125, USA

[4] Research Center for Environmental Changes, Academia Sinica, Taipei 115, Taiwan

Received _____; accepted _____

ABSTRACT

Among the hot Jupiters that transit their parent stars known to date, the two best candidates to be observed with transmission spectroscopy in the mid-infrared (MIR) are HD189733b and HD209458b, due to their combined characteristics of planetary density, orbital parameters and parent star distance and brightness. Here we simulate transmission spectra of these two planets during their primary eclipse in the MIR, and we present sensitivity studies of the spectra to the changes of atmospheric thermal properties, molecular abundances and C/O ratios. Our model predicts that the dominant species absorbing in the MIR on hot Jupiters are water vapor and carbon monoxide, and their relative abundances are determined by the C/O ratio. Since the temperature profile plays a secondary role in the transmission spectra of hot Jupiters compared to molecular abundances, future primary eclipse observations in the MIR of those objects might give an insight on EGP atmospheric chemistry. We find here that the absorption features caused by water vapor and carbon monoxide in a cloud-free atmosphere, are deep enough to be observable by the present and future generation of space-based observatories, such as Spitzer Space Telescope and James Webb Space Telescope. We discuss our results in light of the capabilities of these telescopes.

Subject headings: Atmospheric Effects, Occultations, Radiative Transfer, Techniques: spectroscopic

1. Introduction

Extrasolar Giant Planets (EGPs) are now being discovered at an accelerating pace (Schneider 2006; Butler et al. 2006). In particular, an increasing interest has been focused on hot Jupiters that transit their parent stars, since they represent a valuable tool to determine key physical parameters of the EGPs, such as atmospheric composition and dynamics, thermal properties and presence of condensates (Seager and Sasselov 2000).

The most studied transiting extrasolar planet, HD209458b, orbits a main sequence G-type star at 0.046 AU (period 3.52 days). It is the first one for which repeated transits across the stellar disk were observed ($\sim$ 1.6% absorption; Henry et al. (2000); Charbonneau et al. (2000)). Along with radial velocity measurements (Mazeh et al. 2000), it was possible to determine mass and radius ($M_p \sim 0.69\, M_{Jup}$, $R_p \sim 1.4\, R_{Jup}$), confirming the planet is a gas giant, with one of the lowest densities discovered so far. Owing to this property, its very extended atmosphere is one of the best candidates to be probed with transit techniques. In particular the upper atmosphere extends beyond the Roche lobe, showing a population of escaping atoms. This discovery was possibly due to the observed extraordinary deep absorptions in HI, OI and CII over the stellar emissions lines (15%, 13% and 7.5% respectively; Vidal-Madjar et al. (2003, 2004)). The numerous follow-up observations of HD209458b, also include the detection and upper limits of absorption features in the deeper atmosphere (Charbonneau et al. 2002; Richardson et al. 2003a,b; Deming et al. 2005b; Richardson et al. 2006). Most recently Deming et al. (2005a) detected the thermal emission of this planet with the Spitzer Space Telescope during a secondary transit in the 24 μm band and Richardson et al. (2006) detected the first primary eclipse in the same band.

To explain these observations several models were proposed, including atmospheric photochemistry, thermal properties, 3-D circulation simulations, cloud and condensate height, escaping processes (e.g. Fortney et al. (2003); Burrows et al. (2003); Liang et al. (2003); Lecavelier et al. (2004); Yelle (2004); Tian et al. (2005); Iro et al. (2005); Seager et al. (2005)). For these reasons, the extrasolar planet HD209458b is the best known so far. Additional observations are required, though, to constrain the past, present and future modeling effort.

The planet HD189733b, recently discovered by Bouchy et al. (2005), with mass $M_p \sim 1.15\, M_{Jup}$ and $R_p \sim 1.26\, R_{Jup}$, orbits an early main sequence K star at 0.0313 AU. It is an exoplanet transiting the brightest and closest star discovered so far.

Here we focus our interest on both planets HD209458b and HD189733b, and we model the spectral absorption features in the Mid-Infrared (MIR) due to the most abundant atmospheric molecules during their *primary eclipse*, i.e., when the planet passes in front of the parent star. The use of transmission spectroscopy to probe the upper layers of the transiting EGPs, has been particularly successful in the UV and visible spectral ranges (Charbonneau et al. 2002; Richardson et al. 2003a,b; Deming et al. 2005b;

Vidal-Madjar et al. 2003, 2004), and only very recently attempted in the MIR, in the 24 μm band, using Spitzer observations (Richardson et al. 2006). Two circumstances make it an approach worth considering. First, the high surface temperatures, relatively small masses, and mostly hydrogen atmospheres of close-in EGPs imply large atmospheric scale heights. As a consequence, for spectral features that span a reasonably wide bandwidth, so that the total photon flux is not too small, this is a feasible and diagnostically powerful technique. Second, this is a complementary approach to the secondary eclipse observations. Transmission spectroscopy, taken during primary eclipse, is sensitive to different parameters and regions of the atmosphere, compared to emission spectroscopy, on which the secondary eclipse method is based.

Oxygen versus Carbon → H_2O versus CO In a solar system like ours, a significant amount of water vapor (H_2O) can exist only in planetary atmospheres at orbital distances less than 1 AU. The requirement is certainly met for the known transiting EGPs. Carbon monoxide (CO) and methane (CH_4), and other photochemical products, such as carbon dioxide (CO_2) and acetylene (C_2H_2), are plausibly present in the atmospheres of EGPs, and possibly abundant to be detected. These species have strong absorption bands in the MIR, and more importantly, in spectral regions compatible with present and future space-based observations such as the Spitzer Space Telescope or the James Webb Space Telescope (Gardner et al. 2006). Given O and C, H_2O and CO will be controlled mainly by the relative abundances of these two species.

- If C/O ratio is close to the solar, H_2O, CO and CH_4 abundances are determined by the thermodynamic equilibrium chemistry in the deep atmosphere (Liang et al. 2003, 2004).
- If C/O ratio is above solar, the atmospheric chemistry might change dramatically and, according to the scenario proposed by Kuchner and Seager (2006), planets should show a significant paucity of water vapor in their atmospheres, carbon rich species should by contrast be enhanced. In particular, CO is expected to be the dominant carbon-bearing molecule at high temperatures and CH_4 the dominant at low temperatures (Kuchner and Seager 2006).
- If C/O ratio is below solar, the atmosphere is depopulated of carbon-bearing molecules and water-vapor is the dominant species between $\sim 10^{-10}$ to 1.5 bars.

2. Description of the Model

We have built a model of planetary atmosphere and calculated the expected absorption of the stellar light when filtered through the planetary atmospheric layers. This has

been already discussed in the literature. In particular for our simulations, we have used the geometry and the equations described in Brown (2001) (fig. 1, configuration 2) and Ehrenreich et al. (2006) (sec. 2.1, fig. 1). Our cloud and haze-free atmospheres were divided in forty layers spanning from $\sim 10^{-10}$ to 1 bars.

Photochemical models are used to determine the molecular abundances of 33 species above ∼1 bar altitude level. We start with four parent molecules H_2, CO, H_2O, and CH_4. Their relative abundances are determined by thermochemistry in the deep atmosphere, and are fixed as our lower boundary condition. Chemical reactions and eddy mixing profiles are taken from Liang et al. (2003, 2004). Details of the model can be referred to Liang et al. (2003, 2004) and references contained therein. For the simulation of the photochemistry of HD209458b, we adopt the solar spectrum. For HD189733b we use the spectrum of HD22049, which is a K2V star similar to HD189733 (Segura et al. 2003). We have repeated our calculations for three temperature-pressure profiles (fig. 1 right), to test the sensitivity of our results to these assumptions. The modeled chemical abundances show a negligible dependence on temperature (see (Liang et al. 2004))

The absorption coefficients in the MIR were estimated using a line-by-line model, LBLABC (Meadows and Crisp 1996), that generates monochromatic gas absorption coefficients from molecular line lists -HITEMP, Rothman et al. (in preparation)-, for each of the gases present in the atmosphere.

3. Results

Fig. 1 (left) shows the molecular profiles of H_2O, CO, CH_4, CO_2 and C_2H_2 for both planets HD189733b and HD209458b, calculated by the photochemistry model with solar C/O ratio as boundary condition. On HD189733b, H_2O, CH_4 and C_2H_2 are more abundant in the upper atmosphere compared to HD209458b, since HD189733 is a later type star, therefore the photo-dissociation processes occurring in the atmosphere of that planet are less significant.

Sensitivity to molecular abundances and C/O ratio. Figs. 2 show the predicted absorption signatures due to water vapor and CO on the planets HD189733b and HD209458b. The three plots compare the spectral absorptions of these two species when C/O ratio is solar (standard case, solid line, see fig. 1 left for mixing ratios) and when is below and above solar. As specific examples, we have assumed H_2O to be 10 times more and at the same time CO 10 times less abundant than the standard case (dotted line), and vice-versa (dashed line). When we increase/diminish H_2O and CO of a factor 10, the absorption is increased/decreased by a constant $\sim$ 0.03 % through all the selected wavelength range.

In these figures, we show also the signatures (white rhombi, squares and triangles)

relative to the three cases (standard, C/O ratio below and above solar) averaged over the IRAC, IRS and MIPS bandpasses (centered at 3.6, 4.5, 5.8, 8, 16 and 24 μm), the instruments on board the Spitzer Space Telescope (see table 1 for the calculated absorptions). Water vapor has strong absorption lines through all the selected spectral range in the MIR, the CO signature appears only in a narrower wavelength interval, where the IRAC 4.5 μm bandpass is centered. When the C/O ratio is above solar, the triangle is expected to appear above the rhombus in that band, indicating the strong CO contribution to the total absorption (table 1, numbers in bold).

Note that we included the species CH_4, CO_2 and C_2H_2 in our calculations, which strongly absorb in the MIR. However their abundances are too small compared to CO and H_2O, and they are masked by these species. For example, we show in fig. 3 (left) the contribution due to CO_2 in the case of C/O above solar ratio. CO_2 is increased by a factor 10 here, to follow CO behavior consistently with chemistry predictions (Liang et al. 2003). When CO_2 is present, an increase in absorption of ~ 0.02 % is found in the band centered on 15 μm and a very narrow peak reaching 0.07 % is visible at shorter wavelengths. Although not negligible, the contribution due to CO_2 is masked by CO and water.

Sensitivity to temperature. The effects due to temperature variations (fig. 3 right) are negligible compared to the changes in molecular mixing ratios. Temperature plays a secondary role in the determination of the optical depth: it affects the absorption coefficients and the atmospheric scale heights (see eq. 2 in Ehrenreich et al. (2006)). For HD189733b, the discrepancy between the standard and the hot profile is less than 0.005%, and between the standard and the very hot profile has a maximum of 0.014% in the 15-30 μm range (fig. 3 right). Analogous results are obtained for HD209458b.

4. Discussion

In our model we did not include the contribution of hazes or clouds (Ackerman and Marley 2001; Lunine et al. 1989; Fortney et al. 2005). Due to their presence, the atmospheric optical depth might increase, partially masking the absorption features due to atmospheric molecules. In the case of water vapor and CO, only clouds/hazes lying at altitudes higher than 1 bar might affect our results. Predictions of cloud/haze is particularly difficult for EGPs, since the few observations we have are not sufficient to constrain all the cloud microphysics and aerosol parameters. Moreover, the planetary limb observable during the star occultation might show the signatures of both the night and day side of those planets, which are presumably tidally locked (Iro et al. 2005). The thermal profiles, hence the condensate dynamics, might be very different on the two sides. Consequently, a more complete model able to predict cloud and haze location and optical characteristics, should contain a 3-D dynamical simulation of the atmosphere. In this paper we limit our simulations to the cloud-haze free atmosphere, with the caveat they might be perturbed by

the possible presence (constant or variable) of optically thick particles in the atmosphere above 1 bar pressure.

Same considerations are valid for the thermal profiles. A extensive literature is available on $T-P$ profiles for EGPs at pressures from $\sim$1 bar to 10^{-4}-10^{-6} bars, most recently including 3D dynamical effects (Showman and Guillot 2002; Iro et al. 2005; Cho et al. 2006; Burrows et al. 2006). For transmission spectroscopy in the MIR, we need to consider also the contribution of the upper atmosphere. The $T-P$ profiles calculated by Tian et al. (2005); Yelle (2004) suggest that the trend for the atmospheric temperature is to increase in the exosphere. For our simulations, we use a $T-P$ profile compatible with the lower atmosphere models cited above up to 10^{-3}-10^{-4} bars, and then we consider three cases: the atmospheric temperature decreases up to 10^{-10} bars (standard), the atmosphere is isothermal (hot, very hot profiles). Our results, show that the differences among the spectra calculated with the three profiles are within 0.009 % for $\lambda \leq 14\mu$m and within 0.014 % at longer wavelengths, so we are confident our simulations will not significantly change using a more refined thermal structure.

Our model atmospheres extend to 10^{-10} bars, where non local thermodynamic equilibrium (non-LTE) effects might occur (Kutepov et al. 1998). However, if we truncate our calculations to 10^{-5} bars, we obtain a maximum error of $\sim$ 0.02% at 30 μm (no discrepancy for wavelengths shorter than 20 μm), indicating that our calculated absorptions in LTE regime are correct at first order approximation.

In order to detect the presence of water vapor and CO on HD189733b and HD209458b in the MIR, an extra absorption of $\sim$ 0.15 % is expected to be added to the 2.85 % and 1.6 % due to the optically thick disks at 1 bar atmospheric level. To estimate the chemical abundances, an accuracy of at least 0.03 % is needed. By inspection of the relative absorption of the IRAC 4.5 μm bandpass with respect to the others, we might be able to infer the C/O ratio, but in this case an extremely high S/N is required. HD189733 is a bright K0V star of magnitude K = 5.5. We estimate the brightness in the four IRAC bands to be of the order of 1850, 1100, 730 and 400 mJy at 3.6, 4.5, 5.8 and 8 μm respectively. For HD209458, a G0V star with K-magnitude of 6.3, the IRAC predicted fluxes are 878, 556, 351 and 189 mJy. According to these numbers, a better S/N should be obtainable for HD189733b (Deming et al. 2006), and this makes HD189733b a better candidate for observations.

5. Conclusions

In this paper we have presented simulations of transmission spectra of two extrasolar giant planets during their transit in front of their parent star. According to our calculations, we estimate an excess absorption in the IR of up to 0.15 % for HD189733b and up to 0.12 % for HD209458b (C/O ratio $\sim$ solar), in addition to the nominal 2.85 % and 1.6 %

absorptions measured at shorter wavelengths. If water were far less abundant, other species might be observable, depending on their mixing ratios. Among them, CO_2, CH_4 and C_2H_2 are the best candidates.

According to our simulations, transmission spectra of EGPs in the MIR are sensitive to molecular abundances and less to temperature variations. Temperature influences the transmission spectrum by way of its influence on the atmospheric scale height, as discussed by Brown (2001), and on the absorption coefficients.

If water vapor and CO are as abundant as photochemical models predict, we expect they can be detected with the IRAC, IRS and MIPS instruments on board the Spitzer Telescope and with future telescopes like JWST. Moreover, if an accuracy of 0.03 % is obtainable, future observations may give a first direct estimate of H_2O and CO abundances in the upper atmosphere of EGPs and possibly -depending on their mixing ratios- a constraint on CO_2, CH_4 and C_2H_2.

Acknowledgments

We would like to thank the anonymous referee for his help to improve the paper, L. S. Rothman for having provided the HITEMP data list, R. Ferlet, J. M. Désert, F. Bouchy, G. Hebrard, A. Noriega Crespo and S. Carey, for their valuable inputs, and C. D. Parkinson for useful comments. G. Tinetti is currently sponsored by the European Space Agency. M. C. Liang and Y. L. Yung are supported by the NASA grant NASA5-13296 to the California Institute of Technology.

REFERENCES

Ackerman A.S. and Marley M. S. (2001), ApJ, 556, 872.

Bouchy F., Udry S., Mayor M., Moutou C., et al. (2005), A&A, 444, L15.

Brown T. M. (2001), ApJ, 553, p 1006.

Burrows A., Sudarsky, D., and Hubbard, W. B., (2003), ApJ., 594, 545.

Burrows A., Sudarsky D. and Hubeny I. (2006), ApJ., accepted, astroph 0607014.

Butler R. P., J. T. Wright, G. W. Marcy, et al. (2006), ApJ, 646, 505.

Charbonneau D., Brown T. M.,Latham D. W. and Mayor M. (2000), ApJ, 529, L45.

Charbonneau D., Brown T. M., Noyes R. W. and Gilliland R. L. (2002), ApJ 568, 377.

Cho J. Y. K., Menou K., Hansen B. M. S. and Seager S. (2006), astroph 0607338.

Deming D., Seager S., Richardson L. J. and Harrington J., (2005a), Nature, 434, 740.

Deming D., Brown T. M., Charbonneau D. et al. (2005b), ApJ, 622, 1149.

Deming D., Harrington J., Seager S. and Richardson L. J., ApJ, 644, 560-564

Ehrenreich D., Tinetti G., Lecavelier A. et al. (2006), A&A, 448, 379.

Fortney J. J., Sudarsky D., Hubeny I, et al. (2003), ApJ, 589, 615.

Fortney J. J., Marley M. S., Lodders K., Saumon D. and Freedman R. (2005), ApJ, 627, L69.

Gardner J. P., Mather J. C.; Clampin M. et al., Space Science Reviews, in press.

Henry G. W., Marcy G. W., Butler R. P. and Vogt S.S. (2000), ApJ, 529, L41.

Iro N., Bézard B., Guillot T. (2005), A&A, 436, 719.

Kuchner M. and Seager S. (2006), astroph 0504214, ApJ, submitted.

Kutepov A. A., Gusev O. A., and Ogibalov V. P., 1998, J. Quant. Spectrosc. Radiativ. Transfer, 60, 199-220.

Lecavelier des Etangs A., Vidal-Madjar A., McConnell J. C. and Hébrard G., et al. (2004), A&A, 418, L1.

Liang M. C., Parkinson C. D., Lee A. Y.-T. et al. (2003), ApJ, 596, L247.

Liang M. C., Seager S., Parkinson C. D., et al (2004), ApJ, 605, L61.

Lunine J. I., Hubbard W. B., Burrows A., et al. (1989), ApJ, 338, 314.

Mazeh T., Naef D., Torres G., et al. (2000), ApJ, 532, L55.

Meadows V. S. and Crisp D. (1996), JGR, 101, 4595.

Richardson L. J., Deming D. and Seager S., (2003a), ApJ, 597, 581-589.

Richardson L. J., Deming D., Wiedemann G., et al. (2003b), ApJ, 584, 1053.

Richardson L. J., Harrington J., Seager S. and Deming D., (2006), ApJ, 649, 1043-1047.

Rothman L. S., C. Camy-Peyret, J.-M. Flaud, et al., HITEMP, the High-Temperature Molecular Spectroscopic Database is being prepared for the Journal of Quantitative Spectroscopy and Radiative Transfer.

Schneider J. (2006), The Extrasolar Planets Encyclopaedia, http://exoplanet.eu/

Seager S. and Sasselov D. D. (2000), ApJ, 537, 916.

Seager S., L. J. Richardson , B. M. S. Hansen et al. (2005), ApJ, 632, 1122.

Segura A., Krelove K., Kasting J. F., et al. (2003), Astrobiology, 3(4), 689 -708

Showman, A. P. and Guillot T., (2002), A&A, 385, 166.

Tian F., Toon O. B., Pavlov A. A. and De Sterck H. (2005), ApJ, 621, 1060.

Vidal-Madjar A., Lecavelier des Etangs A., Désert J. M., et al. (2003), Nature 422, 143.

Vidal-Madjar A., Désert J.-M.; Lecavelier des Etangs A. et al.(2004), ApJ, 604, L69.

Yelle R. (2004), Icarus 170, 167.

Table 1. Calculated absorptions averaged over IRAC, IRS & MIPS bandpasses.We recall that 2.85 % and 1.6 % are the nominal absorptions due to the optically thick disks at 1 bar atmospheric level. In bold the absorptions when C/O ratio is above solar and CO strongly contributes in the 4.5 μm IRAC band.

	C/O ratio	3.6 μm	4.5 μm	5.8 μm	8 μm	16 μm	24 μm
HD189733b	< solar	2.953	2.970	3.004	3.001	3.006	3.024
HD189733b	solar	2.930	2.959	2.978	2.974	2.977	2.992
HD189733b	> solar	2.905	**2.961**	2.960	2.952	2.957	2.973
HD209458b	< solar	1.715	1.734	1.773	1.770	1.776	1.796
HD209458b	solar	1.690	1.722	1.746	1.741	1.747	1.766
HD209458b	> solar	1.663	**1.725**	1.724	1.714	1.720	1.738

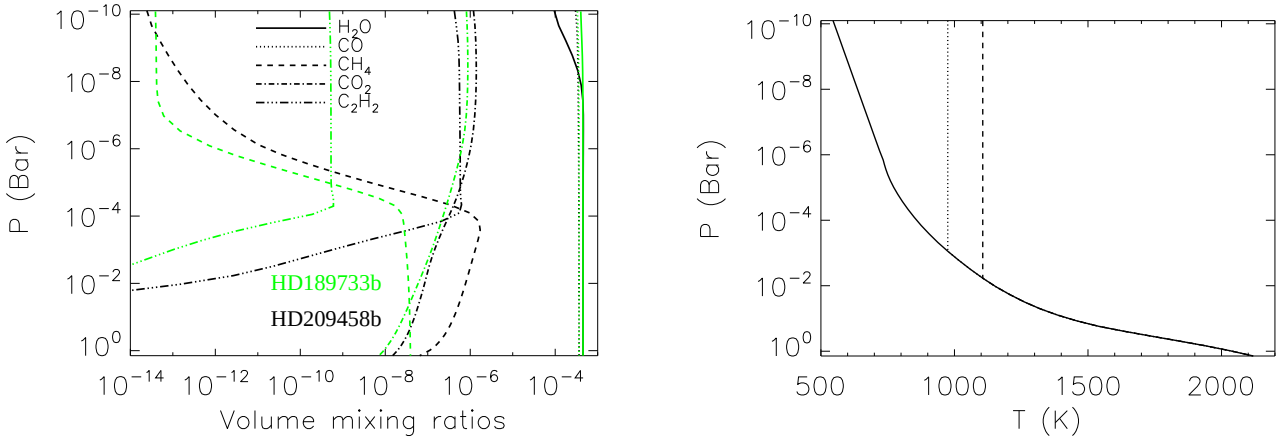

Fig. 1.— Left: Profiles of H_2O (solid line), CO (dotted line), CO_2 (dot-dashed line), CH_4 (dashed line), and C_2H_2 (triple-dot-dashed line) for planets HD209458b (black lines) and HD189733b calculated with the photochemistry model described in Liang et al. (2003, 2004). Right: temperature-pressure profiles used for our simulations. Solid line: standard, dotted line: hot profile, dashed line: very hot profile.

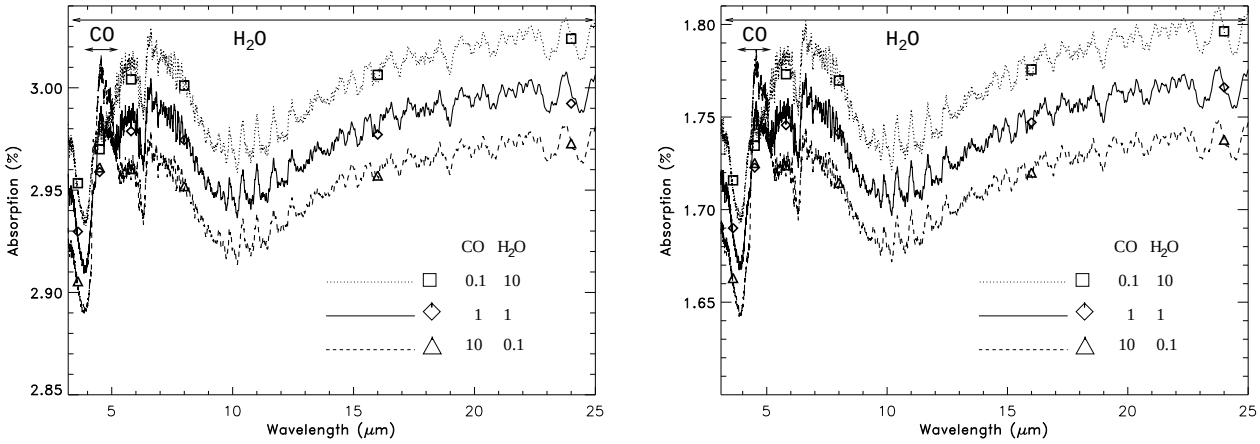

Fig. 2.— Modeled spectral absorptions of water vapor and CO in the atmospheres of HD189733b (left) and HD209458b (right) during their transits. Solid line: standard case, C/O ratio = solar (fig. 1 left); dashed line: CO is over- and H_2O under-abundant of a factor 10; dotted line: the opposite. White triangles, squares and rhombi indicate the spectral absorptions averaged over the Spitzer's IRAC, IRS and MIPS bandpasses, centered at 3.6, 4.5, 5.8, 8, 16 and 24 μm. Only in the 4.5 μm band, where CO shows a strong absorption, the triangle and rhombus overlap.

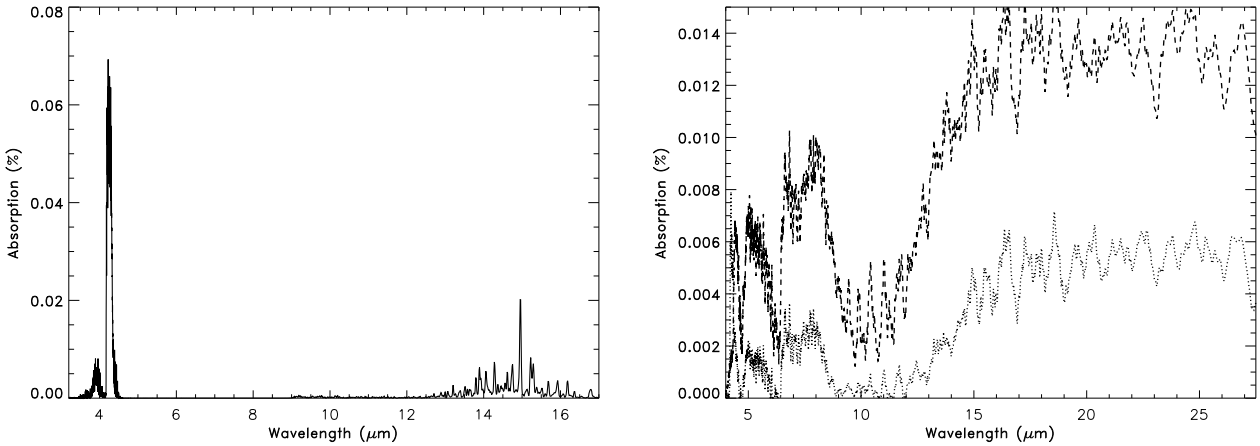

Fig. 3.— Left: residue spectrum from difference of 2 curves: dashed line plot in fig. 2 top with and without the contribution of CO_2. CO_2 is assumed to be, like CO, over-abundant by a factor 10. Right: residue spectra from difference of 2 curves. Dotted line: difference from hot and standard profiles; dashed line: difference from very hot and standard profiles (fig 1 right). The discrepancies amidst the curves is negligible compared to the changes in molecular abundances (fig. 2).